Prifysgol Cymru Abertawe
University Of Wales Swansea

"Going with the flow - Computational Rheology"

Inaugural Lecture

of

Professor Mike Webster

Department of Computer Science

12 November, 2001
Taliesin Arts Theatre

ISBN 0 86076 173 8

First published December 2001, by University of Wales Swansea

Copies obtainable from:

The Department of Planning and Marketing
University of Wales Swansea
Singleton Park
Swansea
SA2 8PP

ISBN 0 86076 173 8

"Going with the flow – Computational Rheology"

Inaugural Lecture/Darlith Agoriadol
12 November 2001

Professor Mike Webster
Department of Computer Science

The title chosen for my lecture today, 'Going with the flow', was coined first by the Government sponsoring agency, Engineering & Physical Sciences Research Council (EPSRC). *Rheology is the science of flowing material - . Computational Rheology implies the study of non-Newtonian fluid flow, via the use of computers.* The two pictures shown illustrate key issues that we shall address: to the left, contrast of rheological properties and response of different fluids, here within splashing experiments; to the right, comparison between simulation and experiment, as in contraction flows.

We begin by setting the scene, with a sample of what you are about to see, relating to non-Newtonian fluids. In fact, this is the trailer for our Institute of non-Newtonian Fluid Mechanics (INNFM) film on the subject - an educational and research tool available in video and CD format, work sponsored by EPSRC under Public Understanding and Awareness. Here, you see some clips for everyday fluids and standard experiments. The multi-media menu sections illustrate the aspects of science involved: Introduction, Viscometry, Rheometry, & non-Newtonian effects; each individually selectable.

By way of introduction, the area of science we pursue leads us to compute solutions (Computer Simulation) to the flows of complex non-Newtonian materials. Domains may be as complicated as required. By complex materials we are referring to their rheological behaviour. Under complicated domains, we mean space (3D)-time, often relating to industrial setting. Hence, we are concerned with pioneering the development of numerical algorithms to solve mathematical problems - themselves models, devised to represent flows in real-life situations (i.e. processing). Typically, such algorithms must translate systems of mixed-type, non-linear partial differential equations, into associated algebraic forms (discretisation), and perform their mechanical solution. This procedure is embodied in computer software (parallel

computation and visualisation), which is implemented on modern computer hardware. Here, we seek tractability for large-scale problems - implying efficiency in computation and speedy turn-round times.

Today, results of our research shall be demonstrated through a series of well-chosen 'Case Studies'. This demands theory beyond that dealing with classical fluid dynamics and takes us from CFD to computational rheology. Hence, we focus upon the complex material within the flow, rather than simpler fluids in complex flows (as in other areas of CFD). First, we need to provide some feel for everyday non-Newtonian fluids, and through illustration, indicate departure from Newtonian behaviour.

An overview of case studies covers both those of a general nature (left) and those of direct industrial relevance (right). Many are clearly recognisable from their title. A selective sample (in bold) will illustrate the many facets of our work and its relevance to modern everyday-life. The geographical co-linearity of the groups within University of Wales INNFM is striking, involving Bangor, Aberystwyth and Swansea. This multidisciplinary Institute (colleagues present in the audience) of mathematicians, engineers and computer scientists, has expanded over the past ten years. It has been recognised as a Centre of Expertise (WDA), and draws down considerable external funding (£3 million, since 1998) from EU, UK government and industry. Over the last year or so, we have had two of our EPSRC research grant proposals, ranked first within the UK. In addition, we have been awarded three consecutive highly-prized "ROPA" awards, specifically targeted at the development of novel research ideas.

From a personal perspective, I was attracted to Swansea in 1986 to form a new research team with Professor Peter Townsend (current Pro Vice-Chancellor & Registrar, Swansea). This meant a return to Wales, where I studied for a PhD in Applied Mathematics at Aberystwyth, a decade earlier, with Professor Ken Walters (FRS) and Professor Russell Davies. As one might gather from the views of Swansea and environs, this is a location of some considerable natural beauty, which is hard to beat and a place that is a pleasure to live and work in.

Over the years, Swansea has had some considerable involvement within this research field, Professor Jim Oldroyd (Mathematics, UWS 1953-65) being a major figure in the

Rheological community and Professor Olec Zienkiewicz (Engineering) in the Finite Element world. There is even some evidence of interaction between these two statesmen of the field. I gathered from private communication with Professor Zienkiewicz, that Oldroyd provided the breakthrough to establishing finite element functions on triangles. This was the mathematical step required to generalise finite element topological reference - and shift consideration from basic brick-shaped (solid) building blocks to those useful in describing deforming matter (liquids). The seminal work of Oldroyd in his Royal Society of London paper (1950), set the scene for constitutive models and the guiding principles for their formulation, to describe material deformation in a generalised framework. This was a contentious issue at the time and somewhat misinterpreted by American colleagues. The classical work in three volumes on finite element methods, of the same name, by Zienkiewicz & Taylor, now enters its fifth edition and remains an authoritative reference in the field. By way of a fairly rough delineation, advances in numerical methods have seen the field shift from finite difference discretisation of the 60's, to finite elements in the 70's, launching finite volume methods 70-80's and spectral methods in the 90's. Such methodology was vital to solve the complex partial differential equations of CFD. Other aspects involved are the choice of variables (streamfunction/vorticity/stress or velocity/pressure/stress) and the level of equations adopted (steady/unsteady and decoupled/coupled).

The tools of the trade, in computing engines through this period have changed beyond recognition, from the mainframes of the 70's, to individual workstations of the mid-80's, to Supercomputers of the early 90's. Today, this has moved onto multi-processor servers and distributed parallel processing with cluster machines. Computer languages have also developed from Algol 60 and FORTRAN of the 60-70's, to Pascal, C and FORTRAN90, and onto High Performance Computing (HPC) of today. Procedural programming has also been challenged by alternative object-oriented, logic, and functional styles. The diversity is clearly apparent.

The simulation software, we have developed, embodies algorithms with finite element and/or finite volume spatial discretisation, in combination with temporal discretisation, to form a stable and accurate time-stepping procedure. Parallel strategies, covering distributed and shared-memory platforms of homogeneous and heterogeneous type,

forge parallelism over many processors. By breaking the full equation system for incompressible flow down into fractional stages, large 3D transient problems are rendered tractable. This encompasses non-Newtonian properties and non-isothermal effects.

Material properties, incorporated within the modelling, include those for constant viscosity (Newtonian) fluids, shear-thinning, strain-hardening and softening fluids, and those that manifest memory effects (viscoelasticity). These properties have been illustrated earlier. In addition, fibre-additives may be accommodated.

Flow geometries of all sorts may be considered, including: two-dimensional (2D) planar, axi-symmetric and three-dimensional (3D) forms. Also, there are those associated with moving fronts or interfaces (such as in injection moulding), and instances where free-surfaces arise (as within extrusion, coating, printing and mixing). Typical finite element meshes in two-and three-dimensional settings are illustrated.

For the mathematically-minded, our modelling may be explained succinctly as follows. The differential equation system is composed of momentum transport and mass balance equations, with an energy equation if non-isothermal, and a constitutive equation for stress. The variables involved are velocity $\boldsymbol{u}$, pressure, p, and stress, □. Non-dimensional numbers of Reynolds and Wiessenberg number (Re and We) govern levels of inertia and elasticity, respectively.

For the numerical analysts present, the principal fe/fv algorithmic framework is that grafted onto a four-staged scheme over a single time-step □t. An iterative loop is then performed to evolve forward in time. Discretisation is implied, over triangles in 2D and tetrahedra in 3D, rendering the fully-discrete matrix-vector system shown - ready for algebraic solution. For viscous incompressible flow, a Taylor-Galerkin scheme (predictor-corrector stage 1a,b) is combined with a pressure-correction scheme (stage 1-3, for incompressibility), that is second-order accurate and semi-implicit in time. Stress (□) is discretised, either in finite-element or volume form. Each approach has its individual merits. Continuous piecewise-quadratic interpolation is adopted for velocity (U) and linear for pressure (P). With the fe-choice, stress interpolation follows

velocity; weighting is of a streamline-type (supg) and superconvergent recovery is applied to velocity gradients. With the fv-form, stress is linearly interpolated on triangular sub-cells within each parent fe-cell. Fluctuation distribution and median-dual-cell constructs are introduced via a cell-vertex approximation. Again, high-order accuracy is achieved.

Returning to 'Case Studies', we begin in some detail with our work on mixing/separating flows, which allows us a backwards, historical glance. This problem is one that manifests both transient and viscoelastic effects. The schematic diagram illustrates the nature of the flow, inflow of the same fluid at two arms, top-right and bottom-left, outflow at the other two locations bottom-right and top-left. A gap in the flow splitter is apparent in the centre. We are able to reflect upon our results published in two Phil. Trans. Royal Society papers, 1980 and 81, demonstrating simulation and experimental observations for increasing flow rates and the significant differences in flow response for Newtonian liquids to some viscoelastic liquids. The gradual appearance of vortices (flow rate increasing down the image) and reversed flow structure is apparent for Newtonian fluids, both via simulation (here) and experiments. These features are absent in the equivalent elastic situations. The simulations at that time were respectable, for Newtonian fluids at least.

We view modern simulations for such a problem, via motion-blur animation sequences. This is a randomised space-filling visualisation technique, which provides a directional feel for the flowing liquids through animation.
First, we look at the transient build-up of flow structure for a Newtonian fluid, commencing from a parallel, but opposing flow scenario. *We ask the question, which way will the flow develop?* Colour is used to indicate strength of flow: red-for-fast, green-medium to blue-for-slow. Now as time advances on the counter, we observe reversed flow developing, and the build-up of a pair of vortices starting at the walls, that merge gradually to a single central vortex. Finally, complete flow reversal dominates. *Second*, for a viscoelastic shear-thinning fluid, we commence from a reverse flow scenario and gradually increase the flow rate. ... At low flow rates, we observe the Newtonian-like response. ... As flow rate increases on the indicator, we begin to see the clear preference for uni-directional viscoelastic flow emerging. At the largest flow rate, there is evidence of die-swell like phenomena, across the gap zone

departing the splitter. Notably, the elastic situation, elusive some twenty years earlier, is now amenable to modern science.

Next, we shift attention to an industrial problem, that of wire-coating, for wires, cables and glass-rovings. Here, pressure monitoring is important to avoid blow-out, and viscoelasticity affects the residual stressing imparted to the coating. Minimal residual stressing is desirable within the cooled working product. This work has been supported by two separate companies over the last ten years, signifying a quarter of a million pounds industrial investment. Here, we seek to understand the fundamentals of the flow process when polymer melts are extruded and drawn onto a fast-moving wire (travelling around 1m/s), to form a coated product for everyday use - i.e. electrical cables. The industrialist would seek to optimise process settings to maintain product quality, maximise output and minimise product wastage. The schema illustrates the polymer coating material, the die geometry and the cable.

Three animation sequences are provided. The first sequence, gives an overview of the industrial extrusion, wire-coating line. The manufacturing line itself may be 200m-300m long. The various components are built-up incrementally, using colour, shading-lighting and movement of parts. The screw extruder, that delivers the molten polymer, is exposed via 3D solid-modelling and sophisticated visualisation techniques. Graphical manipulation allows one to inspect inside the extruder. The second sequence, takes up the next phase and focuses on the wire-coating. We illustrates the wire, the individual distributor and die sections, ..., and the flow of polymer through the geometry onto the cable. Rotation of the viewing angle provides an appreciation of the flow. ... Finally, we zoom into the region identified for simulation. In the third sequence, our numerical predictions are presented for this problem. We begin with the effect of die geometry adjustment. Optimal die positioning avoids unwanted recirculation and pressure blow-out within the die. Note, the rise in pressure, on the scale, as the distributor-tip gets too close to the die-housing. Retraction, too far, reintroduces backflow. *At a fixed die position*, a switch of rheology in the flowing material, from Newtonian to shear-thinning, has the effect of sweeping away the reverse flow (dead zones, where material would degrade). Most severity in the flow occurs at the end of the die, just before the polymer is extruded onto the cable. Stressing in the coating may be picked out, per design, and minimised. A clearer

understanding of these effects has lead to recommendations re optimality of process design for various polymer melt blends. This has lead to improved production and considerable savings through reduction in product wastage. Some static images on field data for pressure, shear-rate and extension-rate, illustrate the distribution of these quantities throughout the flow. Levels of shearing and extension are quadrupled for pressure- above tube-tooling designs.

A second industrial example is that of reverse roller-coating, an investigation into surface instabilities and operating conditions. This work has been sponsored by a local industrial company, Alcoa. Here, the underside of aluminium alloy sheets is coated with a protective layer of solvent-based lacquer (zoomed view). Typically, the coated foil would be used to punch out tin-lids. Processing instabilities (chatter and starvation) generate unevenness in surface finish that is aesthetically unacceptable to the consumer-market. The consequent economic loss due to wastage is considerable. Hence the motivation for the present study: to predict how, when and why such effects arise and to suggest a possible remedy. Printing processes throw up similar scenarios, where product quality and increased throughput are the desired goal.

At this point, we enter a multi-media view of the problem, available over the www. This exposes the high aspect-ratios involved and interrelates the data gathered in a meaningful manner. The alloy foil travels over a tambour roll, and then a series of rollers, that deliver and apply the lacquer to the foil-underside. Foil speed is around 200m/min and the applicator roll-speed is 90% of this. The lacquer coating, without polymer additives, is characterised as a Newtonian fluid. Encapsulating the principal features, a narrow section of the process is analysed: lying from the applicator-roll take-up flow, to the flow between roller and foil, to the surface-coating on the foil. The nip-gap (between roller and foil) and the free-surface meniscus are particularly important.

A parameter sensitivity analysis covers the operating window of applied conditions. We first concentrate on steady flow, with no leakage at the nip. We consider variation in foil-speed at fixed roller-speed. We then invert this test, varying roller-speed at fixed foil-speed. In this fashion, we are able to relate flow and deformation fields to quantities of interest, such as forces upon the foil (lift) and roller (drag). At standard

settings, colour density stream function plots indicate the long thin nature of the flow, ..., that travels from roller, to nip and back to the foil-coating. Pressures and shear-rates are high at the nip. Lift and pressure, localised to the nip (on the right of the graphs), turn out to be important factors in the process. Upon increasing foil-speed, we observe in motion-blur representation (for the meniscus zone), that this draws the flow recirculation closer to the foil and twists the flow lines towards the meniscus. *Interactive interpretation* (through graphs) of corresponding lift and drag, demonstrate the *linear increase in forces* with increasing foil-speed. This is also true of the maxima in shear-rate and pressure at the nip. In contrast, increasing the relative speed of the roller to the foil has the reverse effect. Now, the flow is drawn closer to the roller as its speed increases, and the *forces reflect a linear decrease*. Here, nip shear-rate maxima switch from foil to roller, as roll-speed dominates.

Switching to a temporal analysis, we activate leakage at the nip to act as a flow relief mechanism. The gap at the nip may be widened, by shifting the foil vertically, instigated in a periodic manner. Two aspects have been addressed: the extent of the nip-width widening and the frequency of periodic adjustment (high or low). The extent of the gap-width is found to be a crucial factor in the process. By shifting the whole foil (global) vertically, from 1% to 2% width of coating-flow, nip-pressures fluctuate in time (graphs, p v time) and *temporal surface instabilities* are detected (shown at the top of the screen-shot, against the time-bar). These effects correspond simultaneously with changes in lift. By focusing on lift, per unit length of foil, one observes that maximum lift remains localised to the nip-region, during leakage/no-leakage states. The same is true, but is even more exaggerated, if only a local portion of the foil-length is shifted. The more local the shift, the more the lift is amplified; shown at 30%, 10% and 4% of foil-length shift. Notice the rise in lift to the right of the graphs approaching the nip. This is, in fact, what one might expect in practice. The heart of the problem lies here. We speculate that control of the extent of foil-movement, through appropriate synchronisation mechanisms, will effectively control the surface instabilities.

To add some variety we now switch attention to a rich and varied foods study: that of dough kneading, with applications to bread and biscuit making. The MMS trailer quickly scans what was involved. Five companies (RHM, UB, Pillsbury, Mono

Equipment and SASIB Bakeries) provided industrial trial data and the interdisciplinary research cross-referenced Institute experiments at Aberystwyth with modelling/visualisation at Swansea - a flagship project for the Institute (value £0.75 million, our first BBSRC grant). We were required to: analyse the stirring of dough; gather information on mixer design choice; relate this against dough rheology; predict how to maximise stretching work input to the dough and enhance the build-up of material structure (i.e. kneading). A grand-challenge indeed! This is a key aspect to the overall manufacturing procedure. The work involved: fully-filled and part-filled mixing; steady and unsteady situations; two- and three-dimensional analyses; free-surface movement of the dough; different materials, mixers and configurations.

In the *four images*, we illustrate an empty mixer, two different states of kneading (mixer-lid removed), and a typical final baked product. Commonly, bread mixers are run vertically, biscuit-mixers horizontally. The associated complex free-surface movement involves wetting and peeling on vessel and stirrers - this has demanded new modelling algorithms. Perspective static views of flow patterns are illustrated for a filled one-stirrer mixer with anti-clockwise vessel rotation, shown half-way up the mixer at 50 rpm (a standard speed and model inelastic fluid). Asymmetrical structure is apparent with an off-centre vortex: pressure, shear-rate and rate-of-work extrema are localised to the stirrer. Each menu icon is, in fact, a programmed network (a graph) of the presentation (covering variation in speed, height, material and rotation-type). We contrast this case against the two-stirrer instance: some symmetry is observed about the stirrers and a central figure-of-eight vortex emerges. In three dimensions, we are able to appreciate the depthwise-distribution in rates of shear, extension and work against stirrers and lid.

Animated views, passing through increased speeds, allows the direct cross-reference of simulated data, in pressure, extension-rate and motion-blur fields, against experimental flow visualisation (bottom-left, stirrers indicated). The correspondence in vortex structure is striking. Motion-blur clips at four set speeds of vessel rotation, identify the twisting of the vortex structure with increased speed (in the direction of rotation). This is corroborated in high-speed camera, laser-scatter stills of 1% cmc fluid. At 50 rpm, the motion-blur flow patterns between *one- and two-stirrer mixers* may be contrasted (on the left), whilst also taking the industrialist's view with *stirrers rotating* (on the

right). Next, we turn to the vertical part-filled instance (for bread-making), with a central-stirrer, vessel rotating and compare the final rise surface position graphically against experiment. Agreement is encouraging. Similarly, we may combine cases with three set speeds, 25, 50 and 100 rpm, to demonstrate variation of fluid height-rise at the outer vessel. Such results are obtained by modelling the peeling-off and wetting-onto the surfaces, via the adjustment of surface-fluid line segments, according to their stretch and angle from the solid boundary. Relief of limiting stretch, also relieves critical boundary stress levels. A more complicated vertical scenario is that with a single eccentric stirrer (vessel-rotating). A surface triangulation (heavy on graphics) illustrates the complex shapes encountered. Different viewing angles, with lighting and shading, indicate the surface rise ahead of and dip behind the stirrer. Experimental camera-stills at four different speeds, validate our predictions. There is increased contortion of the surface as speed gathers. The experimental build-up of surface structure is animated from a rest state at 250 rpm vessel-speed.

In contrast, horizontal mixing (used for biscuit-making), may be viewed from one end at four different times. Here, we detect wetting/peeling at the outer vessel and peeling from the stirrer as time progresses. First, we view the simulation through an animation clip. The wetting/peeling at the outer vessel is a dominant feature. This may be contrasted against the corresponding experiment for a syrup at 50 rpm. The surface attachment structure around the inner section of the stirrer and the central flat surface shape are finer detail to capture. Even these particular details may be predicted, by careful localised adjustment of control parameters for the inner and outer stirrer sections (left image, constant factor; right image, dynamic setting).

Lastly, we move to viscoelastic materials, dough-like and filled scenarios. We may observe the stretching and shear stresses across the mixer for a single-stirrer design, or one with a double-stirrer. Maxima in stress are localised about the stirrer, in the narrow-gap between stirrer and vessel; the hoop stress dominates. Tabulations of localised work-input for the double-stirrer case, reveal that elastic work (stretching, shown in red) is dominated by viscous work (shown in blue). Here, shear influences prevail in the totalled work-input. In contrast, the asymmetric single-stirrer design provides ten-times the elastic to viscous work: this is amplified for fluids with some strain-hardening (as occurs with dough). So we arrive at the punch-line: optimal

kneading for dough is achieved with more asymmetrical mixer designs - one stirrer better than two (shades of Orwell). More complex stirrer shapes are usual. In this respect, we observe for realistic dough that flat-bottomed, half-stirrer shapes, produce the best results. Note, the Multi-media presentation style of the future, with personalised, cruise control-navigation, the green panic-button!.

We finish, with a look to the future, and where we are intending to take this technology. A principal plank is our pursuit of quantitative agreement between the modelling and actual fluid flows (experiments). In this respect, we look to such flows as in the contraction, seeking multi-mode and variety of model fits under realistic flow conditions. Here, new challenges are posed to the comparative visualisations sought. Industrial flows abound. Analysis of processing takes us into foods-related studies, for example filament stretching, as arises in deposition of food products (such as yoghurt). Printing and coating of inks is another domain where rheological input is required with the current interest in polymer additives. This brings us naturally to the link between micro- and nano-scale studies, looking at stretching of liquid bridges between surfaces within the realm of biomechanics. A further area of multi-disciplinary interest lies in consideration of compressibility for viscoelastic flows, of relevance within injection moulding. Here, Swansea has a wealth of background knowledge. It is implied that suitable algorithms will be developed to meet the challenges posed by and the individual character of each problem in hand.

I close with thanks. Note, the advanced warning of a second INNFM film (interactive/CD version - top right) on the 'History of Rheology' - the *life and times* of our field. This was constructed with the help of two Olchfa students, Gareth Hunt and David Webster. It shall appear shortly. I am indebted to my research colleagues and students within the team at Swansea and the Institute at large, for their invaluable support and contributions to this body of work.

We finish by playing out on a trailer for our new film ... I thank you once again for your attention.

Mike Webster
12 November 2001

Appendix of slide-images attached.

Appendix I: General slides
Appendix II: Reverse-Roller Coating Multi-media
Appendix III: Dough-Mixing Multi-media

Appendix I: General Slides

Appendix I: General slides

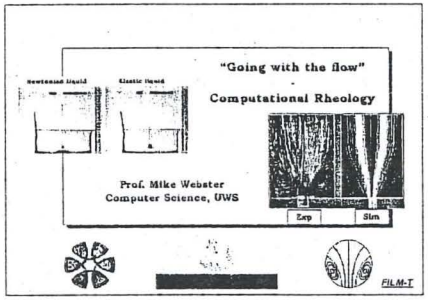

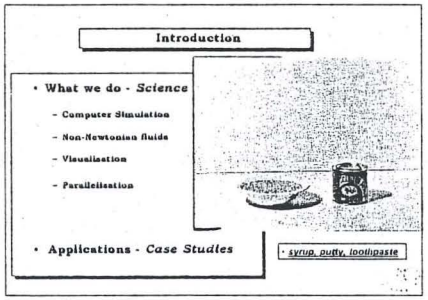

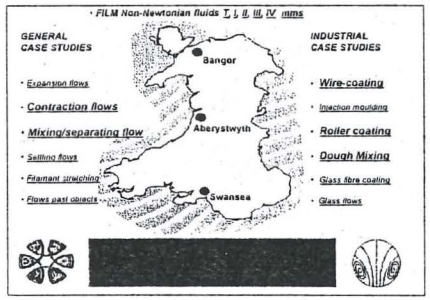

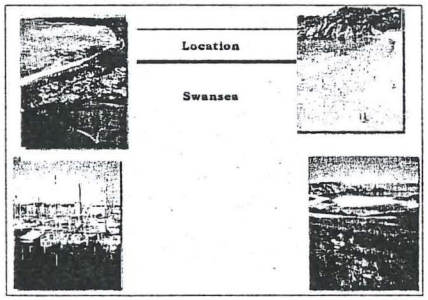

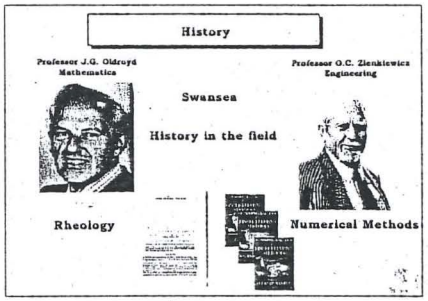

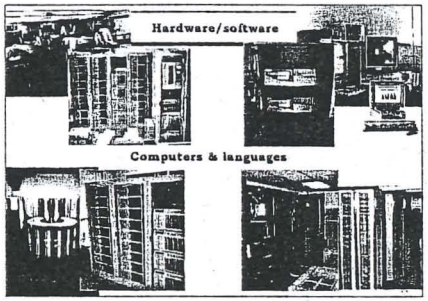

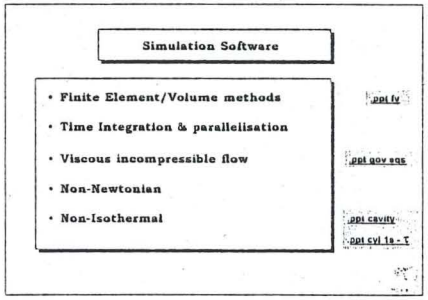

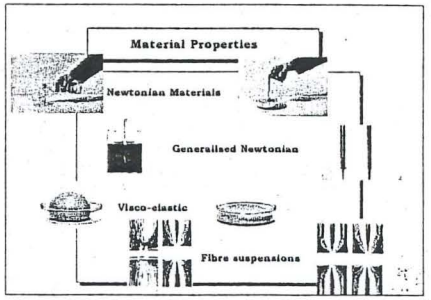

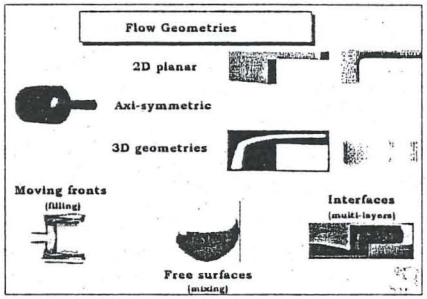

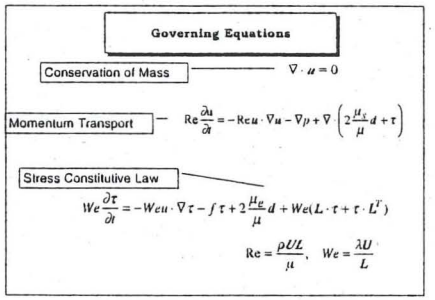

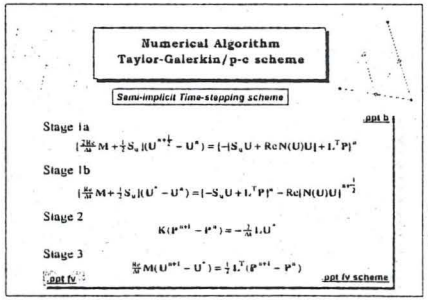

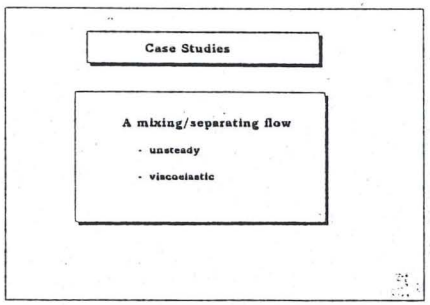

Mixing/Separating Flow

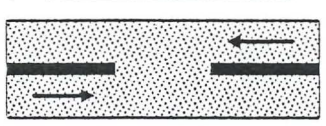

Seq 1: Newtonian, transient build-up & Viscoelastic, increasing flow rate

.ppt 4 slides

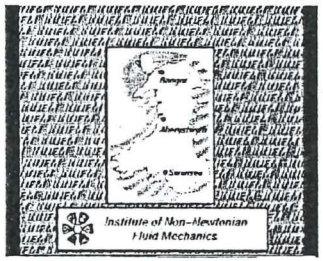

Seq 1: Newtonian, transient build-up & Viscoelastic, increasing flow rate

.ppt 4 slides

Case Studies

Wire Coating

- pressure calculations important
- elasticity important in the design

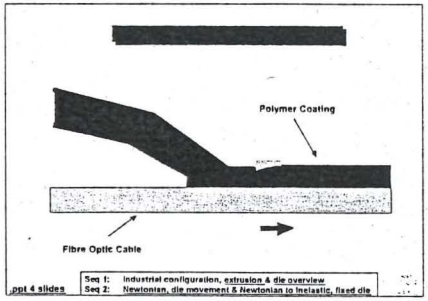

.ppt 4 slides

Seq 1: Industrial configuration, extrusion & die overview
Seq 2: Newtonian, die movement & Newtonian to inelastic, fixed die

Case Studies

Reverse Roller-coating

- free surface instabilities
- optimal operating conditions

Reverse Roller Coating

Multimedia Section

Dough Kneading

Close

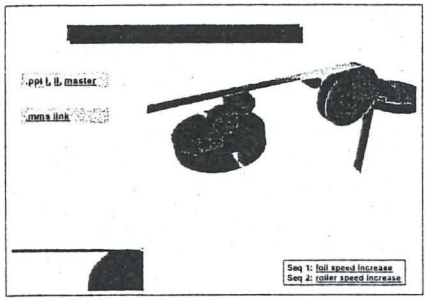

.ppt L ib master

.mms link

Seq 1: foil speed increase
Seq 2: roller speed increase

Case Studies

Dough Mixing

- wetting & pooling bc
- fully filled & part-filled
- transients
- 2D & 3D
- concentric & eccentric stirrers
- different materials & geometries

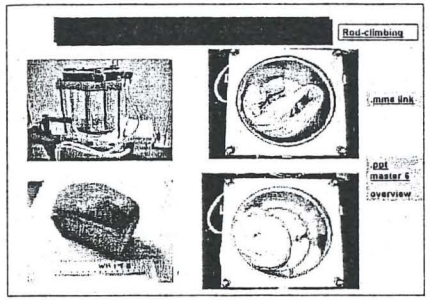

Rod-climbing

.mms link

.ppt master 6

overview

Closing Remarks

- Future
  - Quantitative comparison Simulation v Experiments
  - Contraction flows, multi-mode fluids, other models, transient flows
- Industrial flow
  - Filament stretching (foods)
  - Nano- v micro-scales
  - Printing and coating
  - Incompressible to compressible
- Advance algorithms to suit

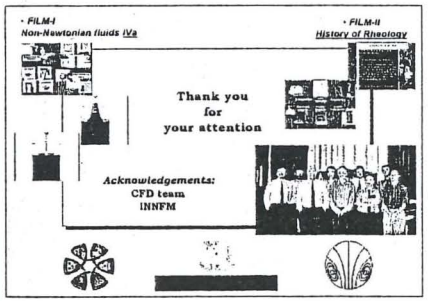

Appendix II:

Reverse-Roller Coating Multi-media

Appendix II: Reverse-Roller Coating Multi-media

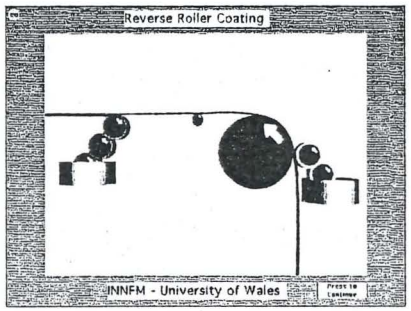

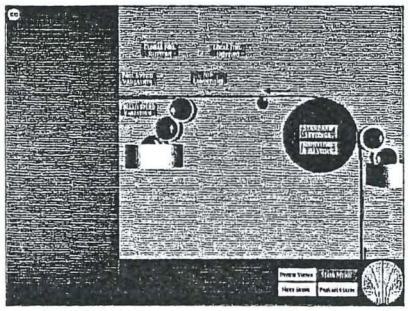

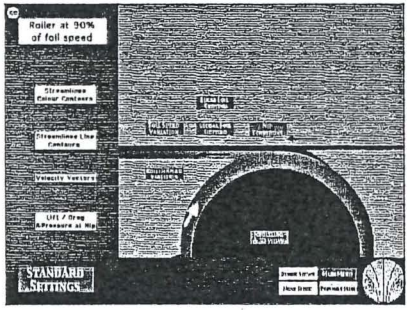

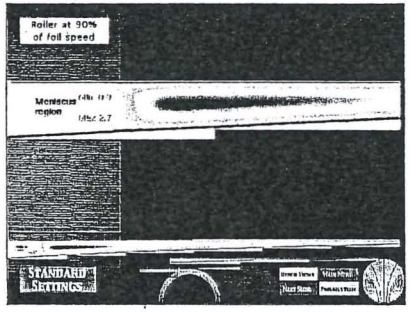

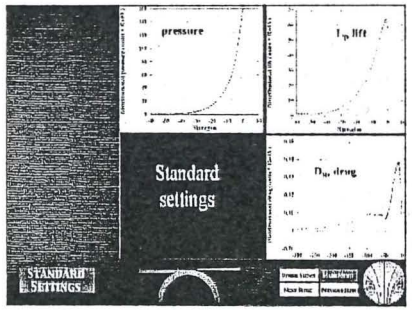

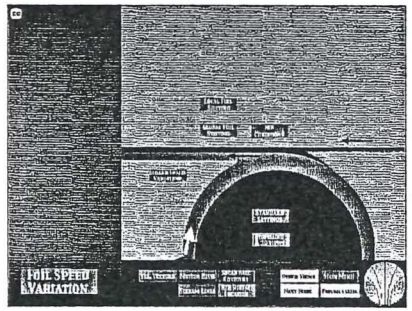

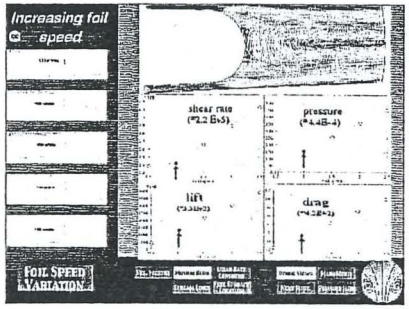

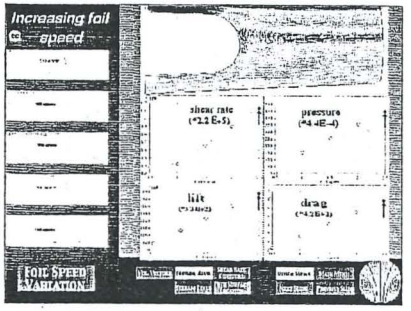

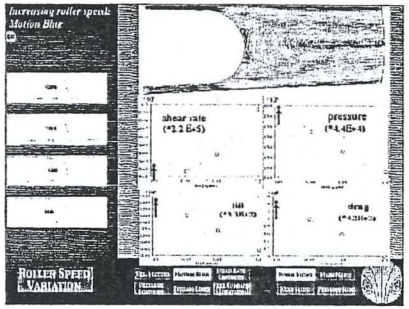

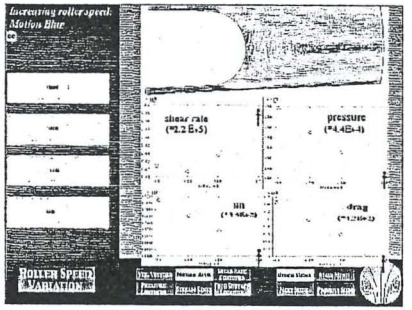

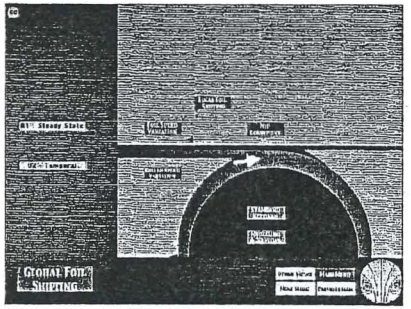

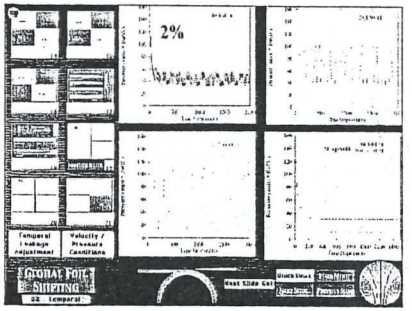

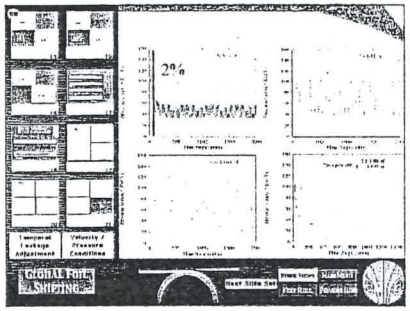

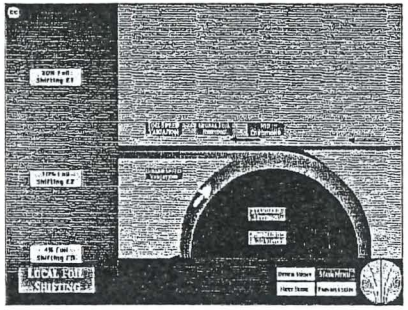

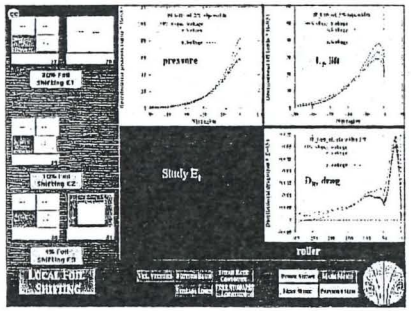

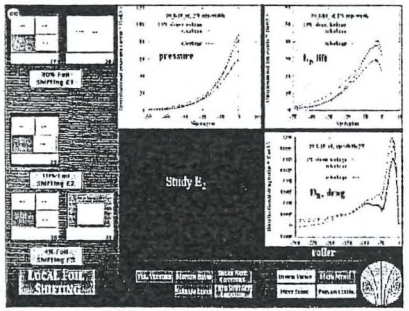

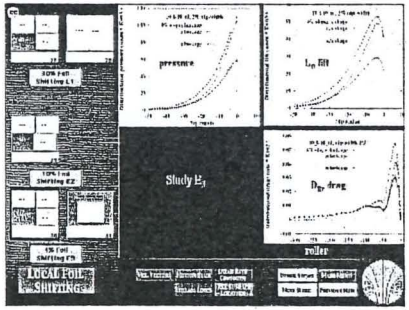

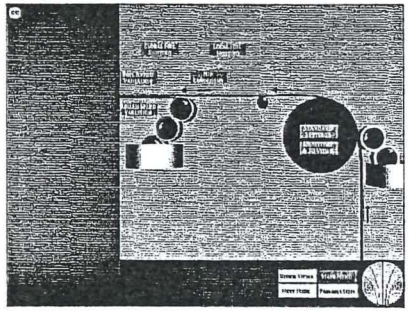

Appendix III:

Dough-mixing Multi-media

Appendix III: Dough-Mixing Multi-media

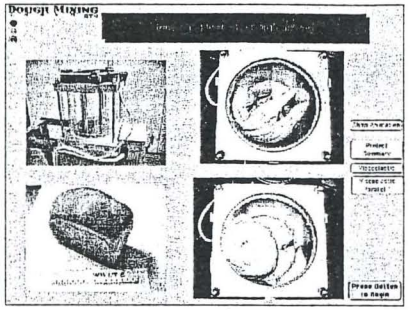

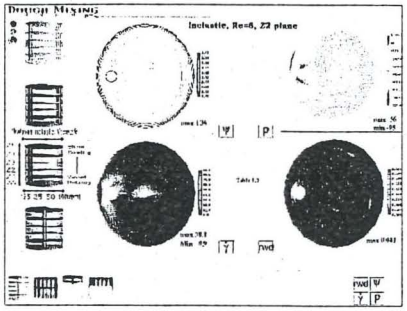

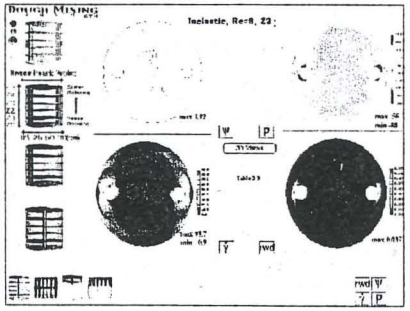

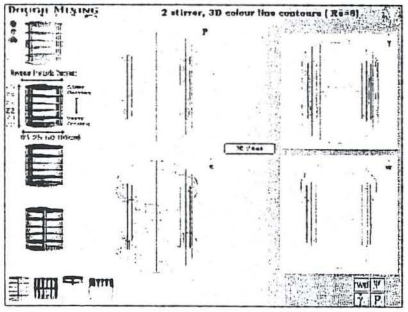

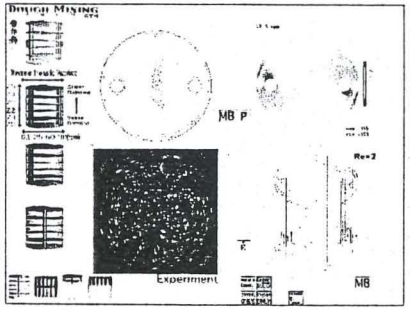

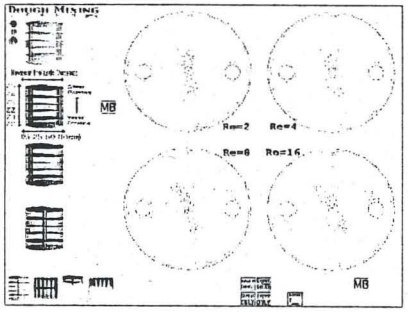

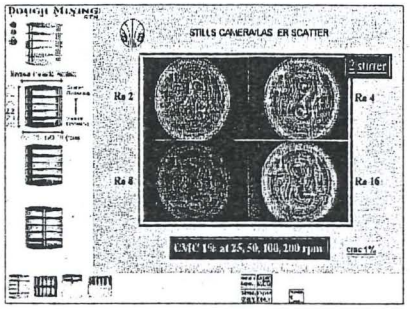

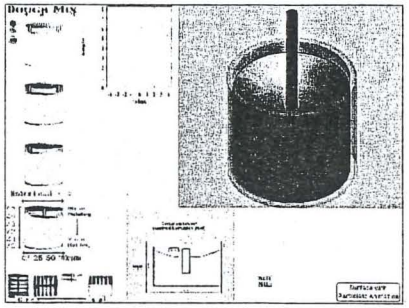

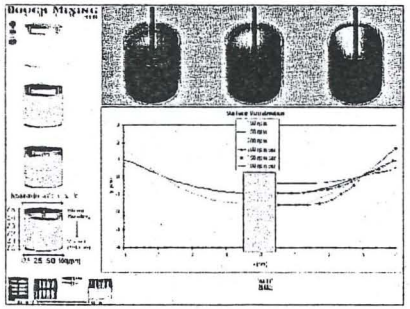

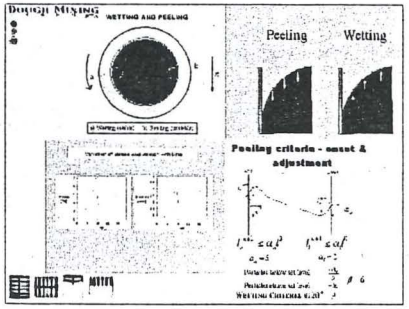

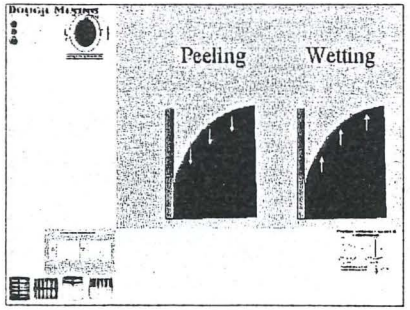

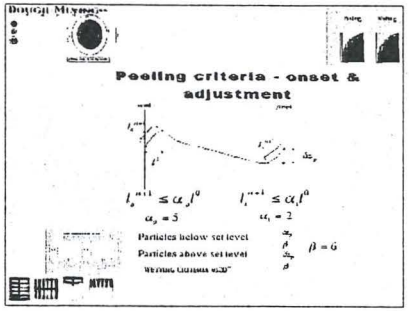

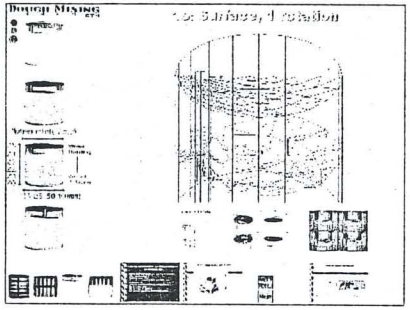

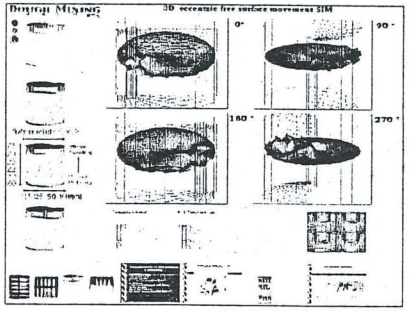

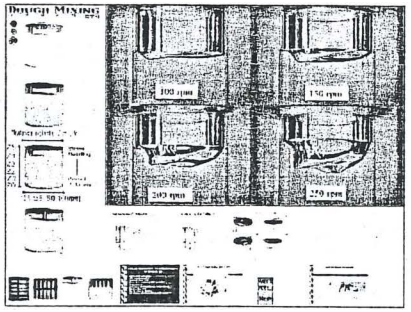

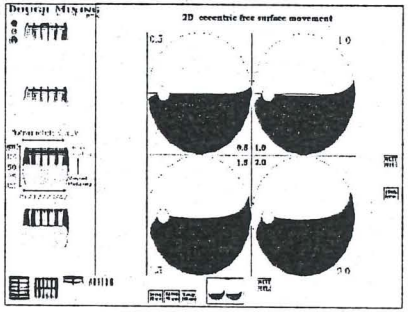

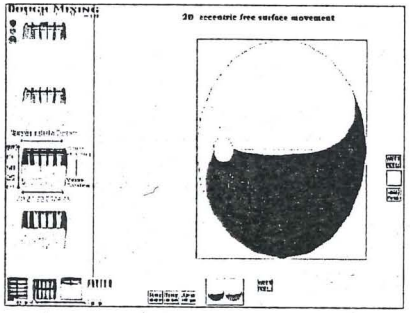

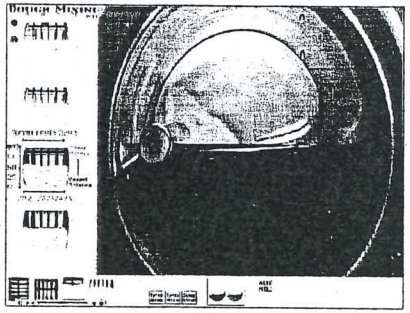

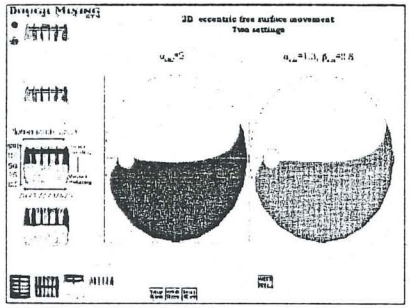

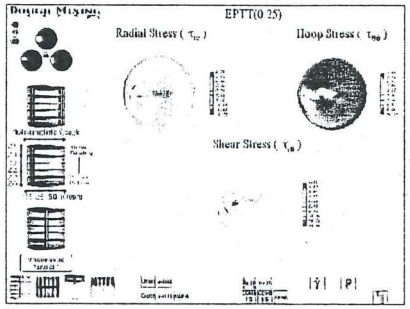

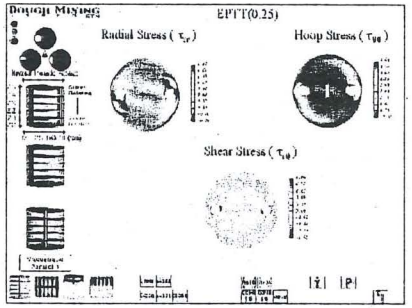

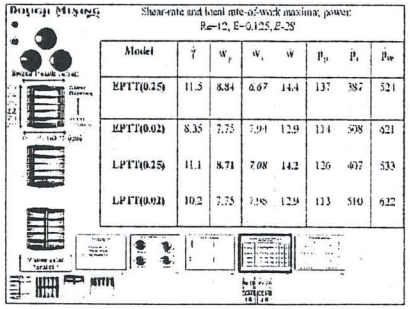

Model	$\dot{\gamma}$	$\dot{W}_{\eta}$	$\dot{W}_{\tau}$	$\dot{W}$	$\dot{P}_{\eta}$	$\dot{P}_{\tau}$	$\dot{P}_{tot}$
EPTT(0.25)	11.5	8.84	6.67	14.4	137	382	521
EPTT(0.02)	8.35	7.75	5.01	12.9	114	508	621
LPTT(0.25)	11.1	8.71	7.08	14.2	126	407	533
LPTT(0.02)	10.2	7.75	5.08	12.9	113	510	622

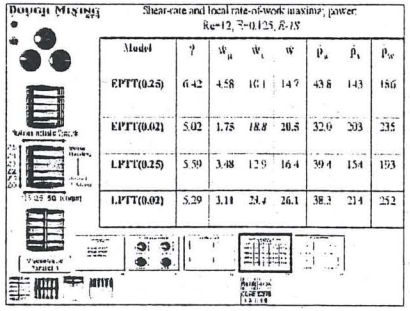

Model	$\dot{\gamma}$	$\dot{W}_{\eta}$	$\dot{W}_{\tau}$	$\dot{W}$	$\dot{P}_{\eta}$	$\dot{P}_{\tau}$	$\dot{P}_{tot}$
EPTT(0.25)	6.42	4.58	10.1	14.7	43.6	143	186
EPTT(0.02)	5.02	1.75	18.8	20.5	32.0	203	235
LPTT(0.25)	5.89	3.48	12.9	16.4	39.4	154	193
LPTT(0.02)	5.29	3.10	23.4	26.1	38.3	214	252